(vinyl group) and the frame behave as rigid units has been assumed as a model for the vinyl group torsion. It is therefore appropriate to use the dihedral angle τ as an internal coordinate for this motion. In order to estimate τ from inertial data, the vinyl group was rotated until the value of Δ_c for the ground state was reproduced. This occurs for $\tau = 13.6°$.

The normal coordinate Q for the vinyl torsion and the dihedral angle τ are related by:

$$Q = (G_{\tau\tau}^{-1})^{1/2}\tau \quad (4)$$

where $(G_{\tau\tau}^{-1})$ is the inverse G matrix element for the coordinate τ.[23] $G^{-1}_{\tau\tau}$ has been calculated for several values of τ and has very little dependence on the angular coordinate. An average value of 10.98 u Å^2 has been used to calculate the value of τ corresponding to the value $\langle\tau_0^2\rangle^{1/2} = 14.7°$.

Using the value of $\tau = 13.6°$ and the assumed structure (see Table IV), the ground-state rotational constants are reproduced with discrepancies of less than 0.3%.

Discussion

The analysis of the microwave spectrum of 2-FS shows the trans form to be the most stable conformer in the gas phase. Careful searches for the microwave spectrum of the cis rotamer were made without success. On this basis the presence of this rotamer cannot be excluded, but if it exists it must be in a very low concentration with respect to the trans form.

Molecules with low-frequency skeletal vibrations often exhibit very anharmonic potential functions. In these cases it is more realistic to give the potential energy function and the corresponding path of motion rather than definite structural parameters. This may be the case of 2-FS for which the microwave data are consistent with a double minimum function contour for the vinyl torsion potential function in the region of the trans rotamer. Moreover, the small barrier to planarity of 16 cm^{-1} separating the two minima corresponding to nonplanar gauche configurations is very close to the lowest vibrational level. In this situation the molecule might be considered vibrating about the planar form even for this vibrational level. We have not sufficient data to perform a complete structural analysis for the path of the vinyl group torsional motion, and so we have only carried out some estimations using a rigid model.

Acknowledgment. The authors express their thanks to Dr. J. M. Hollas for communicating his results and to the Comisiôn Asesora de Investigaciôn Cientifica y Têcnica (CAICYT, Grant PB85-0484) for research support.

Registry No. 2-Fluorostyrene, 394-46-7.

(23) Polo, S. R. *J. Chem. Phys.* **1956**, *24*, 1133-1138.

Gas-Phase Proton Transfer from Toluenes to Benzyl Anions

Chau-Chung Han and John I. Brauman*

Contribution from the Department of Chemistry, Stanford University, Stanford, California 94305-5080. *Received December 2, 1988*

Abstract: Gas-phase proton-transfer kinetics of $PhCH_2^- + ArCH_3 \rightarrow ArCH_2^- + PhCH_3$ were studied for reactions having $\Delta H°_{rxn} = 0$ to -20 kcal/mol. These reactions are very slow in the absence of thermodynamic driving force; their reaction efficiencies range from 0.004 to 0.7. RRKM theory was applied to obtain energy differences between the proton-transfer transition state and the loose orbiting transition state from reaction efficiencies. Marcus theory provides a general model for a rate–equilibrium relationship with a constant intrinsic energy barrier of 7 kcal/mol for the degenerate proton transfer from toluene to benzyl anion. The barrier is inferred from an RRKM fit to the energy difference of -5 kcal/mol between the proton-transfer transition state and the energy of the reactants and an estimated -12 kcal/mol for the energy of the collision complex relative to the reactants. In the reaction involving 3-nitrotoluene, electron transfer, which is some 11–12 kcal/mol less favorable than proton transfer, dominates almost exclusively.

Proton transfers are among the most thoroughly studied reactions. The most widely used free energy relationship, the Hammett equation, is based on acidities of benzoic acids. Rates of exothermic proton transfer reactions in solution vary from diffusion controlled, when the transfer occurs between oxygen and/or nitrogen substrates, to much slower than the diffusion rate, when the reaction involves carbon acids that form delocalized conjugate bases upon deprotonation. Because of the important role of proton transfer in solution chemistry, gas-phase and theoretical studies, particularly thermodynamic properties and reaction dynamics, have vigorously expanded over the past decade in the hope of understanding the intrinsic reactivity and the role of solvent molecules by comparing the behavior to the two phases. Gas-phase kinetic studies have led to conclusions similar to those made for the solution reactions. That is, proton transfers between charge-localized anions proceed with high efficiency[1,2] (close to collision rates) whereas those involving charge-delocalized anions can be slow even when energetically favorable.[1c,3] When only charge-localized anions are involved, it has been observed that some endothermic proton-transfer reactions dominate in the presence of competing exothermic reaction channels if reactant translational energy is enough to overcome the thermodynamic barrier.[4c] On the other hand, although proton-transfer reactions involving charge-delocalized carbon anions have generally been found to be significantly slower than collision rates,[3] they can still be facile enough to be competitive with other exothermic reaction

(1) (a) Bohme, D. K. In *Interactions Between Ions and Molecules*; Ausloos, P., Ed.; Plenum: New York, 1975; p 489. (b) Mackay, G. I.; Payzant, L. D.; Schiff, H. I.; Bohme, D. K. *J. Phys. Chem.* **1976**, *80*, 2919. (c) Nicol, G.; Sunner, J.; Kebarle, J. *Int. J. Mass Spectrom. Ion Processes* **1988**, *84*, 135.

(2) Grabowski, J. J.; DePuy, C. H.; Van Doren, J. M.; Bierbaum, V. M. *J. Am. Chem. Soc.* **1985**, *107*, 7384, and references therein.

(3) (a) Brauman, J. I.; Lieder, C. A.; White, M. J. *J. Am. Chem. Soc.* **1973**, *95*, 927. (b) Farneth, W. E.; Brauman, J. I. *J. Am. Chem. Soc.* **1976**, *98*, 7891. (c) Meyer, F. K.; Pellerite, M. J.; Brauman, J. I. *Helv. Chim. Acta* **1981**, *64*, 1058. (d) Also, see: Bohme, D. K.; Lee-Ruff, E.; Young, L. B. *J. Am. Chem. Soc.* **1972**, *94*, 5153.

(4) (a) Bohme, D. K.; Rakshit, A. B.; Mackay, G. I. *J. Am. Chem. Soc.* **1982**, *104*, 1100. (b) Hierl, P. M.; Ahrens, A. F.; Henchmen, M.; Viggiano, A. A.; Paulson, J. F.; Clary, D. C. *J. Am. Chem. Soc.* **1986**, *108*, 3140. (c) Henchmen, M.; Hierl, P. M.; Paulson, J. F. *J. Am. Chem. Soc.* **1985**, *107*, 2812. (d) Bohme, D. K. In *Ionic Processes in the Gas Phase*; Ferriera, M. A. A., Ed.; Reidel: Boston, 1984; p 111.

0002-7863/89/1511-6491$01.50/0

channels, for example,[5] nucleophilic addition–elimination reactions at a carbonyl center ($B_{AC}2$).

The major shortcoming of the presently available gas-phase techniques is the small dynamic range accessible—reactions that require more than 10^5 collisions to form products cannot be easily studied, mainly due to ion loss as well as to limitations set by reactive impurities.[6] Nevertheless, gas-phase studies within this limited dynamic range have been fruitful and have enabled chemists to better understand solution-phase reactions. Indeed, interest in studying the intrinsic nature of proton-transfer reactions in the absence of solvent molecules has been extended to bridging the gap between unsolvated gas-phase reactions and bulk solution-phase reactions by studying reactivity of partially solvated ions in the gas phase.[1c,4,7]

Farneth et al. studied the kinetics of near thermoneutral proton-transfer reactions between charge-delocalized anions and found that many of them proceed at slow but measurable rates,[3b] with efficiencies ≤ca. 1%. In a later tandem mass spectrometer excitation function study,[8] translational energy thresholds were observed for reactions 1 and 2, which are not expected to behave

$$CH_2{=}CHCH_2^- + C_6H_5CH_3 \rightarrow CH_2{=}CHCH_3 + C_6H_5CH_2^- \quad (1)$$

$$CH_2{=}CHCH_2^- + CD_2{=}CDCD_3 \rightarrow CH_2{=}CHCH_2D + CD_2{=}CDCD_2^- \quad (2)$$

differently from many of the reactions studied by Farneth. Such translational energy thresholds are typical of reactions with energy barriers that are above the separated reactants, and these reactions would have been predicted to be extremely slow (efficiency <ca. 10^{-3}–10^{-4}) at thermal energies. Indeed, these reactions were found to be very slow,[8] in contrast to the previous work in which reaction 1 (exothermic by 11.8 kcal/mol) showed[3a] a thermal energy rate constant of $(7.5 \pm 0.7) \times 10^{-11}$ cm^3 molecule^{-1} s^{-1}. The tandem mass spectrometry excitation function measurements thus appeared to be at varience with the thermal kinetic measurements.[3a,d]

To clarify this problem, we have studied proton transfer from substituted toluenes to benzyl anion, where the thermodynamic driving force can be varied by the substituent introduced. The varying thermodynamic driving force offers a test of the rate–equilibrium relationship, which in turn sheds light on the self-consistency of the kinetic model. The reactions reported in this paper are analogous to reactions 1 and 2. Both the direct reaction rate measurements and the effect of exothermicity on rate constant are found to be consistent with previous thermal kinetic studies.[3]

Experimental Section

Materials. Most chemicals were obtained from commercial sources. Both 3,5-bis(trifluoromethyl)toluene and 3-(trifluoromethyl)toluene were synthesized by preparing the corresponding Grignard reagents from ring-substituted benzyl chlorides followed by quenching with water. 3-(Trifluoromethyl)toluene-α,α,α-d_3 was synthesized from the corresponding ring-substituted benzoyl chloride by reduction with lithium aluminum deuteride in refluxing ether/THF; the product alcohol was then converted into the chloride with thionyl chloride/pyridine and then further reduced with lithium aluminum deuteride. The purity of the deuteriated toluenes were >97% by NMR and deprotonated parent negative ion mass spectrometry. The purity of commercial samples was checked by gas chromatography (GC). Preparative GC or vacuum distillation was used to prepare working samples when purification was necessary.

At the beginning of an experiment, a negative ion mass spectrum was obtained at a long detect delay time (relative to reactant ion generation) to ensure the absence of interfering acid impurities. This was a precaution against the possible contribution from small amounts of acidic contaminants to the observed decay rate of the reactant benzyl anion signal. Since the benzyl anion is a strong base and the near thermoneutral reactions of interest were expected to be rather inefficient, the decay of benzyl anion can be strongly affected by small amounts of acidic impurities that react rapidly with the reactant ion. Contaminants may originate from residues left in the foreline system, and this kind of contamination is independent of purities of reactant samples used.

Instrumentation. A pulsed ion cyclotron resonance spectrometer (ICR) equipped with an elongated cubic cell (1 × 1 × 1.5 in.), a 9-in.-diameter electromagnet (Varian V-3400, operated at 1.2–1.3 T), and a capacitance bridge detector was used for the generation, storage, and mass analysis of the ionic species involved. The pulse sequence and data management routines were controlled by an IBM-PC. The time resolution was set by the detect pulse duration of 8 ms. The detection (ca. 200 mV peak to peak) and double resonance (0.5–2 V peak to peak) signals were provided by separate frequency synthesizers (Hewlett-Packard 3325A and Wavetek 171 respectively).

Trapped thermal electrons were ejected, after the 5–10-ms wide electron beam pulse had been turned off, by applying a 11–13-MHz signal to the trapping plates. During an experiment the pressure of the proton donor was monitored by an ionization gauge (Varian 844) which was calibrated daily against a capacitance manometer (MKS 170 Baratron with a 315BH-1 head) at the end of kinetic runs.

Kinetic Data Collection. The primary ion F^- was generated from dissociative electron attachment to NF_3 (ca. (1–3) × 10^{-7} Torr). Benzyl anion was then generated by the ion–molecule reaction between F^- and benzyltrimethylsilane. When the proton donor (substituted toluene) can be deprotonated by F^-, high partial pressures ((1–3) × 10^{-6} Torr) of benzyltrimethylsilane had to be used, so that F^- preferentially reacted with the silane to generate the reactant benzyl anion rather than with the toluene to produce the product ion directly. This high-pressure condition results in a larger contribution from unreactive ion loss to the measured total reactant ion decay rate. Otherwise, ca. (3–5) × 10^{-7} Torr of the silane was used. In the degenerate proton transfer between 3-$CF_3C_6H_4CH_2^-$ the reactant ion was generated from deprotonation of the corresponding toluenes by F^-. A mixture of the protio and deuterio forms of the anions is formed at the ratio of the parent neutral molecules. At the time (with respect to the electron beam pulse) when $C_6H_5CH_2^-$ reached its maximum, the remaining F^- was ejected from the cell, and the kinetic data collection routine was started.

The temporal pseudo-first-order decay of the $C_6H_5CH_2^-$ signal was monitored and signal averaged 10–30 times at each incremental time delay while the product $XC_6H_4CH_2^-$ was continuously ejected by double-resonance ion ejection. Resonance shifts were corrected for by scanning the radio-frequency signal generator across the resonance peak to obtain the strongest signal reading at each detect pulse time delay before the signal readings were stored and processed. The decaying signals of $C_6H_5CH_2^-$ over 3.5–5.0 half-lives were displayed in a semilog fashion to facilitate the detection of deviations from pseudo-first-order kinetics. The slope of the linearly distributed data points (typically consisting of 10–15 equally spaced points), after correction had been made for unreactive ion loss (vide infra), gave the pseudo-first-order reaction rate constant. All reactions were studied at ambient temperatures of 350 ± 5 K, measured by a fine wire thermocouple (Omega) attached to the Vespel frame on which the cell plates were fixed.

Reaction 3 represents a generalized gas-phase proton transfer between two anions. The contribution from the unreactive ion loss to the measured total ion decay rate constant is accounted for when the experimental pseudo-first-order rate constant, k_{obsd}, is converted into the second-order reaction rate constant, k_2, according[10] to Scheme I. Un-

Scheme I

$$I_t(A^-) = I_0(A^-)\exp(-k_{obsd}t)$$

$$k_{obsd} = k_{1L}(A^-) + k_2[B]$$

$$k_2 = \frac{k_{obsd} - k_{1L}(A^-)}{[B]}$$

(5) (a) Holtz, D.; Beauchamp, J. L.; Woodgate, S. D. *J. Am. Chem. Soc.* **1970**, *92*, 7484. (b) Beauchamp, J. L. In *Interactions Between Ions and Molecules*; Ausloos, P., Ed.; Plenum: New York, 1975; p 413.

(6) For example, in studying nucleophilic substitution reactions of carbanions with methyl bromide, traces of HBr in the sample result in the facile production of Br^- due to proton transfer to the strongly basic carbanions. Contamination may also originate from the sample inlet system.

(7) However, the relevance of reactions involving partially solvated ions in the gas phase to solution reactions have been questioned, because the gas-phase reactions frequently do not or only partially transfer the solvent molecules to the product ion, whereas ionic species are always completely solvated in solution. See: (a) Henchman, M.; Paulson, J. F.; Hierl, P. M. *J. Am. Chem. Soc.* **1983**, *105*, 5509. (b) Hierl, P. M.; Ahrens, A. F.; Henchman, M.; Viggiano, A. A.; Paulson, J. F. *J. Am. Chem. Soc.* **1986**, *108*, 3142. (c) Also see ref 4c.

(8) Lifshitz, C.; Wu, R. L. C.; Tierman, T. O. *J. Am. Chem. Soc.* **1978**, *100*, 2040.

(9) Bartmess, J. E.; McIver, R. T., Jr. In *Gas Phase Ion Chemistry*; Bowers, M. T., Ed.; Academic: New York, 1979; Vol. 2.

(10) Unreactive ion loss is a nearly first-order process at low pressures (being a very weak function of pressure) and becomes second order at higher pressures. See: Farneth, W. E. Ph.D. Thesis, Stanford University, 1975. At a given pressure the kinetics of unreactive ion loss can be characterized by a pseudo-first-order rate constant k_{1L}.

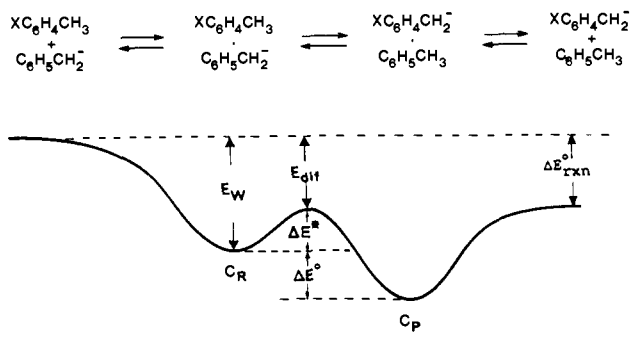

Figure 1. Double-minimum potential energy surface model for gas-phase proton transfer between benzyl anions. E_{dif} and E_W as shown are defined as negative quantities.

reactive ion-loss rate constants were measured without applying double-resonance ion ejection. For a reversible, near thermoneutral reaction, where the reactant ion signal has significant intensity at equilibrium, the decay of the reactant ion due to unreactive ion loss was monitored directly. For a nonreversible or an exothermic reaction, the pseudo-first-order unreactive ion-loss rate constant of the product ion, $k_{1L}(B^-)$, was obtained by monitoring the decay of B^- after all the A^- had reacted or after reaction 3 had reached equilibrium. The pseudo-first-order ion-loss

$$A^- + BH \xrightarrow{k_2} AH + B^- \qquad (3)$$

$$\frac{k_{1L}(A^-)}{k_{1L}(B^-)} = \frac{1}{P_{AX} + P_{BH} + P_C} \frac{M_A^{1/2}}{M_B^{1/2}} \left\{ P_{AX} \frac{\mu_{BAX}^{1/2}}{\mu_{AAX}^{1/2}} + P_{BH} \frac{\mu_{BBH}^{1/2}}{\mu_{ABH}^{1/2}} + P_C \frac{\mu_{BC}^{1/2}}{\mu_{AC}^{1/2}} \right\} \qquad (4)$$

rate constant for A^-, $k_{1L}(A^-)$, was then estimated from $k_{1L}(B^-)$ by using[11] eq 4, where P_{AX} and P_{BH} are the partial pressures of the precursors for A^- and B^-, respectively, and P_C represents the partial pressure of NF_3. μ_{ABH}, etc., are the reduced masses of the corresponding colliding ion–neutral (A^- and BH) pairs.

Data Analysis

A double-minimum potential energy surface model,[3,12] Figure 1, can rationalize the reaction kinetics observed. According to this model, the separated reactant acid–base pair, $XC_6H_4CH_3$ and $C_6H_5CH_2^-$, are the most energy-rich species on the adiabatic reaction potential energy surface. Upon collision they form a complex (C_R) that is stabilized by charge–dipole and charge–induced dipole interactions. C_R is similar to the reactants and is separated from a second productlike complex ion, C_P, by an energy barrier that arises from transferring the proton from $XC_6H_4CH_3$ to $C_6H_5CH_2^-$. The barrier is necessarily lower in energy than the separated reactants; otherwise, the reaction rate would be too slow for us to measure.

At the 10^{-7}–10^{-6} Torr of total pressure typically employed in this study, the lifetime of the chemically activated collision complex ion is so short (estimated to be ≤ca. 10^{-6} s) that collisional relaxation (occurring on a millisecond time scale) does not occur, but long enough so that complete energy randomization can be assumed and the behavior of the decomposing complex ions (both C_R and C_P) can be predicted by statistical unimolecular reaction theories. The statistical theory of our choice is the RRKM theory[13] (the quasiequilibrium theory of mass spectrometry). The details of the RRKM analysis have been described previously[14] and will not be repeated here.

The proton-transfer transition state is entropically unfavorable, because the C–H–C bonding has turned the free rotational motions of the separated reactants into vibrations. Thus, the barrier, while lower in energy than that of the separated reactants, effectively retards a reaction. A calculated reaction efficiency is determined by convoluting the correct energy distribution function with the fraction of the sum of states of the proton-transfer transition state and the orbiting transition state leading C_R to the regeneration of the reactants.[12,13] The ratio of sums of states, in turn, is a function of the differences in energy, E_{dif}, and the vibrational frequencies and moments of inertia of the two transition states. In the RRKM calculations, vibrational frequencies and moments of inertia of the transition states are chosen by using the corresponding parameters for related species or by making estimates;[14] thus, E_{dif} becomes the only adjustable parameter. With a chosen set of molecular parameters for the two transition states, the "experimental" E_{dif} is determined as that calculated value that reproduced experimental reaction efficiency in the RRKM calculation. The energy barrier to proton transfer, ΔE^*, can be obtained from E_{dif} if the stability of the reactant complex with respect to the separated reactants, E_W^R, is known.

The choice of RRKM input parameters follows the same principles used previously.[14] Briefly, the loose orbiting transition state is modeled as composed of a benzyl anion and a substituted toluene molecule at a separation of 7.4–7.7 Å and as if each were unperturbed by the presence of the other. The vibrational frequencies for $C_6H_5CH_2^-$ are approximated by those of aniline,[15,16] which is isoelectronic with benzyl anion. The tight proton-transfer transition state is modeled as a pair of (substituted) benzyl anions bonded through a proton bridge with the two aromatic rings in a parallel conformation separated by[17] 3 Å. In going from the loose to the tight transition state, four free rotations of the fragments become rocking motions with assumed frequencies of 200 cm^{-1}; in the combination of two benzyl anions and a proton to form the tight proton-transfer transition state, three additional new internal vibrations are created: one symmetric stretch[18] at 300 cm^{-1} and two bends[19] involving the bridging proton at 1200 cm^{-1}. The asymmetric stretch involving the three moieties in $XC_6H_4CH_2$–H–$CH_2C_6H_5$ corresponds to the reaction coordinate. Disregarding substituents that do not change upon reaction such as CF_3, there are two one-dimensional rotors (CH_3 in the toluene, and the relative rotation of the fragments around the intermolecular axis that gives rise to an "effective" one-dimensional rotor) and two two-dimensional rotors in the loose orbiting transition state. Only the "effective" one-dimensional rotor is retained in the tight transition state, and it is treated with a reduced moment of inertia.[14,20]

For a homologous series of reactions, a rate–equilibrium relationship exists if all reactions follow the same mechanism and if the transition states bear resemblance to the reactants and products.[21] Thus, one can predict reaction rates, based on kinetic

(11) This is based on an equation derived by Olmstead; see: Olmstead, W. N. Ph.D. Thesis, Stanford University, 1978; p 95–100.
(12) (a) Olmstead, W. N.; Brauman, J. I. *J. Am. Chem. Soc.* **1977**, *99*, 4219. (b) Asubiojo, O. I.; Brauman, J. I. *J. Am. Chem. Soc.* **1979**, *101*, 3715.
(13) (a) Forst, W. *Theory of Unimolecular Reactions*; Academic: New York, 1973. (b) Robinson, P. J.; Holbrook, K. A. *Unimolecular Reactions*; Wiley-Interscience: New York, 1972.
(14) (a) Pellerite, M. J.; Brauman, J. I. *J. Am. Chem. Soc.* **1980**, *102*, 5993. (b) Pellerite, M. J. Ph.D. Thesis, Stanford University, 1981.
(15) Evans, J. C. *Sepctrochim. Acta* **1960**, *16*, 248.
(16) The bending and stretching vibrations of the NH_2 functional group of aniline will have somewhat different frequencies from those in the CH_2 functional group of benzyl anion, but the differences are not expected to affect the results, since these are mostly high-frequency vibrations (thus do not contribute as much to the sums of states as low-frequency vibrations) and their contributions to the sums of states of the two transition states partially cancel.
(17) The optimum H–C distance between the transferring proton and the benzyl carbon in the tight transition state is estimated at 1.47–1.61 Å by semiempirical quantum mechanical MNDO calculations with the two aromatic rings fixed to be parallel to each other and with different relative orientations around the intermolecular axis. The C–H distances in the transition state for symmetric proton transfers between saturated carbon anions are calculated to be 1.42–1.47 Å. See: (a) Wolfe, S. *Can. J. Chem.* **1984**, *62*, 1465. (b) Latajka, Z.; Scheiner, S. *Int. J. Quantum Chem.* **1986**, *29*, 285. An intermediate value of 1.5 Å is used for simplicity. The results of the RRKM calculations are insensitive to slight changes in this separation as long as the vibrational frequencies are fixed.
(18) Estimated from the symmetric vibrational frequency of proton bound dimer of NH_3 (668 cm^{-1}) by making correction for the difference in masses between NH_3 and C_7H_7.
(19) Estimated by analogy with the degenerate bending frequencies found for HF_2^-.
(20) The effective and reduced moments of inertia for the one-dimensional rotors of reaction pairs reported in Table I (in the corresponding order) are as follows: 279, 181; 414, 234; 370, 217; 475, 252; 373, 215; 842, 611, respectively (in units of amu·Å^2).

Table I. Proton-Transfer Rate Constants, Reaction Efficiencies, Reaction Energetics, and E_{dif} for $XC_6H_4CH_2^- + YC_6H_4CH_3 \rightarrow YC_6H_4CH_2^- + XC_6H_4CH_3$

X	Y	k_2[a]	efficiency[b]	$-\Delta H°_{rxn}$[c]	$-E_{dif}$[d]
H	D_8[e]	0.05 ± 0.02	0.004 ± 0.002	~0	5.0 ± 0.4
H	3-CF_3	1.3 ± 0.1	0.07 ± 0.01	11.5	8.3 ± 0.1
H	3-CN	0.5 ± 0.1	0.022 ± 0.005	11.5	8.4 ± 0.3
H	3,5-$(CF_3)_2$	12.0 ± 1.0	0.68 ± 0.06	19.8	11.8 ± 0.3
H	4-CN	9.2 ± 0.9	0.39 ± 0.06	19.8	11.4 ± 0.4
3-CF_3	3-CF_3-D_3[f]	0.43 ± 0.05	0.028 ± 0.003	~0	8.0 ± 0.1

[a] k_2, the experimental second-order reaction rate constant, expressed in units of 10^{-10} cm^3 $molecule^{-1}$ s^{-1} and measured at ambient temperature of 350 K. The uncertainties reflect the reproducibility on different days and represent 1 standard deviation of the results. [b] Reaction efficiency = k_2/k_{ADO}, where k_{ADO} is the theoretical ion–molecule collision rate constant predicted by the average dipole orientation (ADO) theory; see ref 28. [c] kcal/mol; data from ref 26. [d] E_{dif}, the energy difference between the proton-transfer transition state and the reactants at infinite separation obtained by RRKM simulation. The uncertainty reflects the error in experimental reaction efficiency. [e] Perdeuteriated toluene. [f] Deuteriation at the benzylic position.

data obtained for any member in the series, for other reactions for which only thermodynamic information is available. The Marcus equation,[22] eq 5, has been shown to be of great value because of the insight it provides into intrinsic reactivity and of its simplicity, generality, and predictive power.[14,23]

$$\Delta E^* = \Delta E_0^* + \frac{\Delta E°}{2} + \frac{(\Delta E°)^2}{16\Delta E_0^*} \quad (5)$$

The Marcus formalism applies to the complex-to-complex (i.e., C_R to C_P) elementary process and relates ΔG^* to $\Delta G°$, which is the energy difference between C_P and C_R, instead of the overall $\Delta E°_{rxn}$. This practice may be problematic not only because of the paucity of experimental information on E_W but also because of the possibility of involving peculiar interactions that exist only in C_R and/or C_P but not in the reactants and/or proton-transfer transition state (or vice versa). This suggested the re-formulation of the Marcus equation by defining the separated ion–neutral molecule pairs (instead of C_R and C_P) as the reactant and product in an elementary reaction.[24] The re-formulated Marcus equation, eq 6,

$$E_{dif} = E°_{dif} + \frac{\Delta E°_{rxn}}{2} + \frac{(\Delta E°_{rxn})^2}{16(E°_{dif} - E_W)} \quad (6)$$

is similar in form to the original equation but it allows one to use the overall reaction energy change, $\Delta E°_{rxn}$ rather than the complex-to-complex energy change, $\Delta E°$. This is an advantage when the well depths of C_R and C_P are expected to be significantly different and direct measurements are not available. In our case, the thermodynamic driving force in the reactions arises from introducing substituents into the toluene molecule. A change in dipole moment and polarizability accompanies the substitution and therefore E_W^R and E_W^P (E_W's for C_R and C_P, respectively) are expected to be significantly different. As a result, $\Delta E°$ is not equal to $\Delta E°_{rxn}$ in general, and the correct usage of eq 5 is not straightforward when only the overall reaction energy change is available. Thus, the reformulated form, eq 6, will be used in the rate–equilibrium relationship analysis.

In using eq 6, E_{dif} and E_W are both defined as negative quantities if the corresponding species, the proton-transfer transition state and C_R, respectively, are lower in energy than the separated reactants. In addition, eq 6 is applicable only over the range of $\Delta E°_{rxn}$ given by $|\Delta E°_{rxn}| \leq 4(E°_{dif} - E_W)$.

In applying eq 6, we have taken, in the absence of experimental data, E_W to be −12 kcal/mol; 10–15 kcal/mol is a common binding

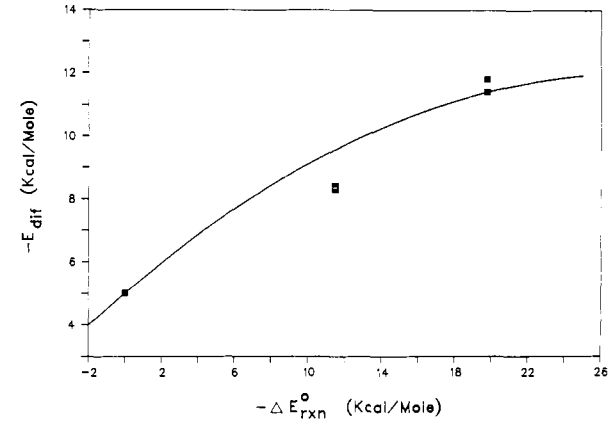

Figure 2. Correlation of E_{dif} with $\Delta E°_{rxn}$ for $XC_6H_4CH_3 + C_6H_5CH_2^-$. Points: experimental E_{dif} values obtained from RRKM simulation of experimental reaction efficiencies. Curve: functional dependence of E_{dif} on $\Delta E°_{rxn}$ predicted by eq 6 with constant $E°_{dif}$ = −5 kcal/mol, which was obtained for $C_6H_5CH_2^-$.

energy found in dimeric aromatic cluster ions bound only by nonspecific interactions.[25] In addition, the "experimental" E_{dif} values listed in Table I (vide infra) fall in the range that eq 6 is valid. Equation 6 is derived for a double-minimum surface, and the exact value for E_W is generally not crucial.[24] The binding energy for E_W in the $C_6H_5CH_2^-·C_6H_5CH_3$ complex is likely to be less than 12 kcal/mol due to the low dipole moment of toluene and the delocalized charge in benzyl anion. However, since $\Delta H°_{rxn}$ (or $\Delta E°_{rxn}$) = 0, the last term in eq 6 vanishes for all nonzero values of $E°_{dif} - E_W$.

Results

Reaction rate constants, efficiencies, energetics, and $-E_{dif}$ are summarized in Table I. The uncertainty in bimolecular reaction rate constants, k_2, reflects the reproducibility of the reported values on different days and represents 1 standard deviation of the results. It is seen that four values were reproducible to within 10%, one within 20%, and one degenerate reaction within 40%. All reactions are significantly slower than the collision limit, even for the most exothermic reaction reported. The effect of thermodynamic driving force on the reaction efficiency is clearly seen from the results summarized in Table I. Reaction exothermicity accelerates the reaction by increasing $-E_{dif}$, as predicted by eq 6.

Preliminary results on reaction 7, which is exoergic by[26] 28.4 kcal/mol, indicate a reaction efficiency of ≤85%. An attempt was made to measure the rate constant for proton transfer from 3-$NO_2C_6H_4CH_3$ to $C_6H_5CH_2^-$, but interestingly, only electron transfer was observed. Neither of these results is included in Table I.

$$C_6H_5CH_2^- + 4\text{-}NO_2C_6H_4CH_3 \rightarrow C_6H_5CH_3 + 4\text{-}NO_2C_6H_4CH_2^- \quad (7)$$

Discussion

The results summarized in Table I indicate that proton-transfer reactions between benzyl anions have significant intrinsic activation barriers. While a thermodynamic driving force is seen to accelerate the reactions, the effect is quite weak and consistent with a large intrinsic energy barrier based on the analysis of eq 6. To test the applicability of the Marcus equation, we took the values E_W = −12 kcal/mol (vide supra) and $E°_{dif}$ = −5 kcal/mol (the value obtained for $C_6H_5CH_2^- + C_6H_5CH_3$; see Table I). Then, a functional dependence of E_{dif} on $\Delta E°_{rxn}$ can be obtained from eq 6, which is shown as the smooth curve in Figure 2. In applying eq 6, we assumed that the frequency changes on going to the

(21) Hine, J. *J Org. Chem.* **1966**, *31*, 1236.
(22) Marcus, R. A. *J. Phys. Chem.* **1968**, *72*, 891.
(23) (a) Pellerite, M. J.; Brauman, J. I. *J. Am. Chem. Soc.* **1983**, *105*, 2672. (b) Pellerite, M. J.; Brauman, J. I. In *Mechanistic Aspects of Inorganic Reactions*; Rorabacher, D. B., Endicott, J. F., Eds.; ACS Symposium Series No. 198; American Chemical Society: Washington, D.C., 1982; Chapter 4.
(24) Dodd, J. A.; Brauman, J. I. *J. Phys. Chem.* **1986**, *90*, 3559.
(25) Examples of specific interactions include hydrogen bonding and resonance stabilization.
(26) Lias, S. G.; Bartmess, J. E.; Liebman, J. F.; Holmes, J. L.; Levin, R. D.; Mallard, W. G. Gas-Phase Ion and Neutral Thermochemistry. *J. Phys. Chem. Ref. Data* **1988**, *17*, Suppl. 1.

proton-transfer transition state are the same for each of the reactants. That assumption is not exact, since the $\Delta S°_{rxn}$ is not identical for these compounds, but the error introduced by this is relatively minor. The experimental E_{dif} values agree well with the predicted ones at the corresponding reaction exothermicity as is seen in Figure 2. This agreement suggests that these reactions have similar reaction dynamics and intrinsic energy barriers.

Although the fit shown in Figure 2 implies a constant intrinsic barrier, we studied a second degenerate reaction, (8), as a cross check. The $-E°_{dif}$ obtained from the RRKM simulation of the experimental reaction efficiency was 8 kcal/mol, 3 kcal/mol larger than that obtained for $C_6H_5CH_2^- + C_6H_5CH_3$. A ca. 1 kcal/mol scatter of experimental data points about the smooth theoretical curve is noted in Figure 2. This scatter may well be an indication of the uncertainty in the extraction of a rate constant from the experimental data. A 3 kcal/mol deviation from the theoretical line for the $3\text{-}CF_3C_6H_4CH_2^- + 3\text{-}CF_3C_6H_4CD_3$ seems large, but it may have arisen from experimental errors difficult to circumvent. This has to do with the double-resonance ion ejection technique. At 1.2 T, the resonance frequency of the reactant ion, $3\text{-}CF_3C_6H_4CH_2^-$, differs from that of the product ion, $3\text{-}CF_3C_6H_4CD_2^-$, by only 1440 Hz. The reaction rate was obtained by monitoring the pseudo-first-order decay of the reactant ion while a continuous double-resonance signal tuned to the resonance frequency of the product ion is applied. Since the difference in resonance frequency between the two isotopically labeled ions is so small, it is possible that the reactant ion is also affected by the double-resonance ion ejection signal and an artificially faster reaction rate constant is obtained under such conditions. In contrast, the difference in resonance frequency for $C_6H_5CH_2^-$ and $C_6H_5CD_2^-$ is 4330 Hz at the same magnetic field. A possible alternative method for collecting kinetic data by observing the establishment of equilibrium after a pulsed double-resonance ejection of the product ion is also difficult, due to the competing unreactive ion loss with the slow reaction. Thus, because of the good fit of experimental data points by eq 6, as shown in Figure 2, and the possibility of experimental error in the rate constant measurement for reaction 8, we believe that the intrinsic energy barrier in the series of proton-transfer reactions between benzyl anions are essentially constant and that the Marcus equation provides satisfactory predictive power for these reactions. In general, we might expect small differences in the intrinsic barriers.[27] More reaction rate measurements for the degenerate reactions will undoubtedly help to clarify the 3 kcal/mol difference in E_{dif} found for the two degenerate reactions studied.

Since E_{dif} is obtained from the experimental reaction efficiency, it is important to establish the accuracy of k_{ADO}, the estimated collision rate constant based on the average dipole orientation (ADO) theory.[28] For this purpose, we studied reaction 7, which is exoergic by 28.4 kcal/mol and thus predicted to be a near-collision-limited reaction by eq 6, to see if the rate constant for a highly exoergic reaction is still limited by k_{ADO}. Unfortunately, it was difficult to achieve good reproducibility in the rate constant measurements for reaction 7. This was probably due to the low vapor pressure of this compound so that traces of a (relatively) high vapor pressure contaminant left in the foreline system from previous experiments significantly affected the pressure measurement. Nevertheless, the upper limit to the reaction efficiency obtained on 10 different days converged at ca. 85%. This, and all the other results listed in Table I, may be taken as suggesting

$$3\text{-}CF_3C_6H_4CH_2^- + 3\text{-}CF_3C_6H_4CD_3 \rightarrow 3\text{-}CF_3C_6H_4CH_2D + 3\text{-}CF_3C_6H_4CD_2^- \quad (8)$$

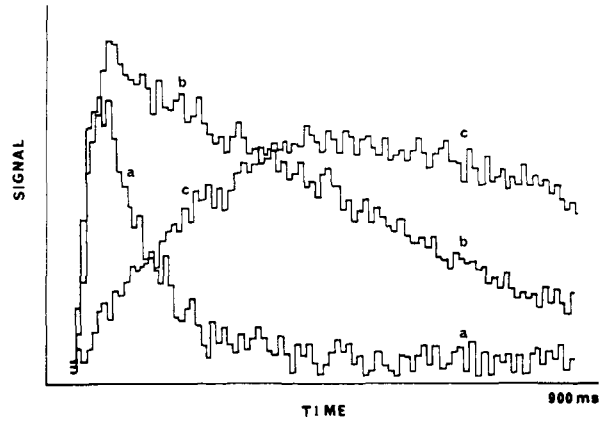

Figure 3. Variation of ion populations as a function of time in $C_6H_5CH_2^-$ + $3\text{-}NO_2C_6H_4CH_3$: (a) $C_6H_5CH_2^-$; (b) $3\text{-}NO_2C_6H_4CH_2^-$; (c) $3\text{-}NO_2C_6H_4CH_3^-$. $C_6H_5CH_2^-$ was initially generated from $F^- + C_6H_5C\text{-}H_2Si(CH_3)_3$; $3\text{-}NO_2C_6H_4CH_2^-$ is shown to be initially generated from deprotonation of $3\text{-}NO_2C_6H_4CH_3$ by F^-. Electron transfer is seen to be the dominant reaction channel. Partial pressures of NF_3, $C_6H_5CH_2Si\text{-}(CH_3)_3$, and $3\text{-}NO_2C_6H_4CH_3$ were 3×10^{-7}, 11×10^{-7} and 1×10^{-7}, Torr respectively.

that the theoretical ion–molecule collision rate constants predicted by the ADO theory,[28] k_{ADO}, are reasonable upper bounds to the reaction rates.

A second purpose for choosing $4\text{-}NO_2C_6H_4CH_3$ as the proton donor was because of the extraordinarily high degree of charge delocalization of its conjugate base. The Kochs concluded in a solution study that the carbanion $XC_6H_4C^-(H)(CF_2OCH_3)$, where X = CH_3, CH_3O, H, F, Cl, Br, or NO_2, is highly delocalized only when X = $4\text{-}NO_2$, whereas the charge remains largely localized on the benzylic carbon in the other carbanions.[29] If so, peculiar kinetics may be observed when the gas-phase proton-transfer reaction involves a similarly charge-delocalized benzyl anion $4\text{-}NO_2C_6H_4CH_2^-$. Unfortunately, the scatter in our rate constant measurements could not provide us a chance to analyze the reaction. Nevertheless, $4\text{-}CNC_6H_4CH_3$, another possible (but not as good as $4\text{-}NO_2C_6H_4CH_3$) candidate for showing particularly high degrees of charge delocalization in the conjugate base, reacts normally.

The observation that electron-transfer reaction predominates in $C_6H_5CH_2^- + 3\text{-}NO_2C_6H_4CH_3$, Figure 3, suggests that the corresponding electron-transfer reaction is much faster than proton transfer and thus has a lower or negligible activation barrier. This is also consistent with the presence of significant energy barriers in the proton-transfer reaction, considering that proton transfer[26] is some 16–17 kcal/mol more exothermic than electron transfer.[30] This may suggest[31] a reaction mechanism where the observed proton-transfer channel is a result of a fast electron-transfer reaction (operative when the electron affinity of the proton donor is higher than that of $C_6H_5CH_2^-$) followed by a rate-determining hydrogen-atom-transfer step. In most reactant pairs the hydrogen atom transfer is sufficiently fast due to overall exothermicity and is the observed reaction channel. Only when the overall reaction exothermicity is such that the hydrogen-atom-transfer transition state is not sufficiently stable to compete with the fragmentation of the electron-transfer intermediate does one observe this energetically less favorable electron-transfer channel. Because of the strong binding of the electron in the benzyl anion and the relatively small (and possibly nonpositive) EA of some of the neutral toluenes, however, it is very unlikely that this is a general reaction path for all substrates. For these reactions,[30,32] $EA(C_6H_5CH_2)$ = 19.9 kcal/mol, $EA(3\text{-}NO_2C_6H_4CH_3)$ = 21.4 kcal/mol, and

(27) For a discussion of the effects of gradually changing intrinsic barriers, see: Lewis, E. S.; Douglas, T. A.; McLaughlin, M. L. In *Nucleophilicity*; Harris, J. M., and McManus, S. P., Eds.; American Chemical Society: Washington, D.C., 1987; Chapter 3.

(28) Su, T.; Bowers, M. T. In *Gas Phase Ion Chemistry*; Bowers, M. T., Ed.; Academic Press: New York, 1979; Vol. 1, Chapter 3. The treatment of Su and Chesnavich [Su, T.; Chesnavich, W. J. *J. Chem. Phys.* **1982**, *76*, 5183] does not give significantly different values.

(29) Koch, H. F.; Koch, J. G.; Koch, N. H.; Koch, A. S. *J. Am. Chem. Soc.* **1983**, *105*, 2388.

(30) Grimsrud, E. P.; Caldwell, G.; Chowdhury, S.; Kebarle, P. *J. Am. Chem. Soc.* **1985**, *107*, 4627.

(31) Han, C.-C.; Brauman, J. I. *J. Am. Chem. Soc.* **1988**, *110*, 4048.

(32) Drzaic, P. S.; Brauman, J. I. *J. Phys. Chem.* **1984**, *88*, 5285.

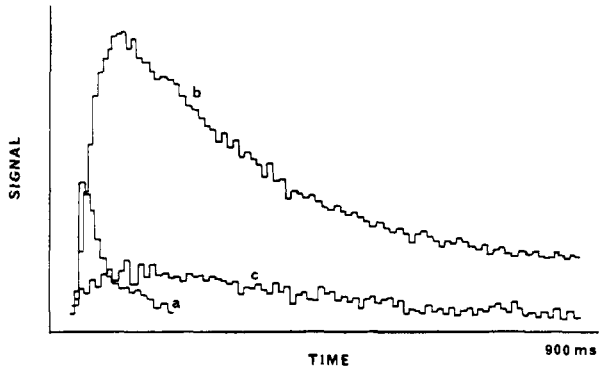

Figure 4. Variation of ion populations as a function of time obtained under similar conditions as Figure 3 but continuous double-resonance ejection of $C_6H_5CH_2^-$ is applied here: (a) F^-; (b) $3\text{-}NO_2C_6H_4CH_2^-$; (c) $3\text{-}NO_2C_6H_4CH_3^-$.

$EA(4\text{-}NO_2C_6H_4CH_3) = 20.5$ kcal/mol.

Owing to the generation of $3\text{-}NO_2C_6H_4CH_2^-$ from deprotonation of $3\text{-}NO_2C_6H_4CH_3$ by F^- and the experimental difficulty involved when ion ejection and detection of ions of the same mass is carried out on our instrument, we have not been able quantitatively to determine the amount of $3\text{-}NO_2C_6H_4CH_2^-$ formed from proton transfer to $C_6H_5CH_2^-$. In a separate experiment with the same bath gas composition as that used in obtaining Figure 3, $C_6H_5CH_2^-$ was ejected throughout the duty cycle. It is seen in Figure 4 that $3\text{-}NO_2C_6H_4CH_2^-$ reaches its maximum at the same time F^- disappears. This indicates that the $3\text{-}NO_2C_6H_4CH_2^-$ observed in Figure 3 originates mainly (or exclusively) from deprotonation of the parent neutral moleules by F^- rather than by $C_6H_5CH_2^-$, since the latter is ejected in obtaining Figure 4. In Figure 4, only a trace of $3\text{-}NO_2C_6H_4CH_3^-$ was detected, and it was further shown to have originated from direct attachment of unejected thermal electrons by observing similar amounts of $3\text{-}NO_2C_6H_4CH_3^-$ in the absence of NF_3 and $C_6H_5CH_2Si(CH_3)_3$. Thus, the results shown in Figure 4 indicate that reaction 9 is very slow, consistent with its expected endothermicity.

$$3\text{-}NO_2C_6H_4CH_2^- + 3\text{-}NO_2C_6H_4CH_3 \rightarrow 3\text{-}NO_2C_6H_4CH_2^{\bullet} + 3\text{-}NO_2C_6H_4CH_3^{\bullet -} \quad (9)$$

In reaction 7, a small amount (up to ca. 10% of the proton-transfer product) of electron transfer was detected when no double-resonance ion ejection was applied. The molecular radical anion $4\text{-}NO_2C_6H_4CH_3^{\bullet -}$ can also be shown to have originated exclusively from direct attachment of unejected thermal electrons to the parent neutral molecules by its persistent existence when $C_6H_5CH_2Si(CH_3)_3$ is pumped out or $C_6H_5CH_2^-$ is ejected. Thus, electron transfer from $C_6H_5CH_2^-$ to $4\text{-}NO_2C_6H_4CH_3$ is also inferred to be slow relative to the proton-transfer reaction.

Isotopically labeled toluenes were used in the degenerate reactions eq 10. Therefore, possible isotope effects should be

$$ArCH_2^- + ArCD_3 \rightarrow ArCD_2^- + ArCH_2D \quad (10)$$

considered. If we assume a correction factor[33] of 2 to our rate constants for thermoneutral reactions, the corrected rate constants for the reverse reaction are still much smaller than k_{ADO}, and it is clear that the kinetic isotope effect is not going to cause any problem in analyzing the data. First, the real thermoneutral, degenerate reaction will have a rate constant intermediate between the two extreme values corresponding to the reactions in the forward and reverse directions for the quasidegenerate reaction and is thus within our experimental uncertainty. Second, the effect due to differences in zero-point energy is partly taken into consideration in the RRKM analysis by using appropriate frequencies for the isotopically labeled molecules. Third, for a slow reaction, the largest uncertainty lies in the measured rate constant due to unreactive ion loss and pressure measurement, making small corrections for kinetic isotope effects relatively unimportant. Fourth, the rate constant measured here for $C_6H_5CH_2^- + C_6D_5CD_3$ is in good agreement with the value obtained earlier for $C_6H_5CH_2^- + 4\text{-}DC_6H_4CH_3$ by Lieder.[34] $(3 \pm 1.5) \times 10^{-12}$ molecule^{-1} cm^3 s^{-1}, where the isotope effect is negligible. Finally, tunneling is not expected to be a serious concern, because the energy of the chemically activated collision complex is well above the barrier to proton transfer between the two benzylic sites.[35,36]

In summary, we have confirmed that proton transfer from toluene to benzyl anion is about 0.4% efficient, in agreement with earlier ICR[3a] and flowing afterglow[3d] work and in contrast to tandem mass spectrometric results,[8] which indicated a much slower reaction. Using a double-well-potential model, we suggest that the transfer of a proton from a toluene molecule to a benzyl anion in the gas phase involves a transition state that is ca. 5 kcal/mol more stable than the reactants. This corresponds to a 7 kcal/mol intrinsic energy barrier (ΔE^*_0) with respect to the intravening and even more stable loose ion–molecule complexes when a well depth, $E_W = -12$ kcal/mol, is assumed. The resulting double-minimum potential energy surface can rationalize the observed reaction kinetics. The rates of exothermic proton transfers from substituted toluene molecules to the benzyl anion can be predicted by the Marcus equation with a constant intrinsic energy "barrier" of $E^\circ_{dif} = -5$ kcal/mol. Thus, proton-transfer reactions involving charge delocalized carbanions are slow in both solution and the gas phase. However, the interesting observation that charge delocalization alone is not sufficient to make a proton-transfer reaction slow[37] has not been tested by gas-phase studies.

Acknowledgment. We are grateful to the National Science Foundation for support of this work. We thank Professor R. W. Taft for providing us acidities of substituted toluenes before publication.

(33) This can be seen by applying eq 6 to the cross reaction $C_6H_5CH_2^- + 3\text{-}CF_3C_6H_4CH_3$. This reaction behaves normally and can be fit into the same rate–equilibrium relationship as the others.

(34) Lieder, C. A. Ph.D. Thesis, Stanford University, 1974.

(35) Scheiner, S.; Latajka, Z. *J. Phys. Chem.* **1987**, *91*, 724.

(36) A theoretical study has concluded that proton tunneling is unimportant in nondegenerate proton-transfer reactions because of additional symmetry requirements; see: de la Vega, J. R. *Acc. Chem. Res.* **1982**, *15*, 185.

(37) Kresge, A. J. *Acc. Chem. Res.* **1975**, *8*, 354. However, for a recent discussion of resonance delocalization in some common ions, see: Siggel, M. R.; Thomas, T. D. *J. Am. Chem. Soc.* **1986**, *108*, 4360. Wiberg, K. B.; Laidig, K. E. *J. Am. Chem. Soc.* **1988**, *110*, 1872.